

Finite-size scaling above the upper critical dimension

Matthew Wittmann¹ and A. P. Young^{1,2}¹*Department of Physics, University of California, Santa Cruz, California 95064, USA*²*Max Planck Institute for the Physics of Complex Systems, Nöthnitzer Strasse, 01187 Dresden, Germany*

(Received 21 October 2014; published 29 December 2014)

We present a unified view of finite-size scaling (FSS) in dimension d above the upper critical dimension, for both free and periodic boundary conditions. We find that the modified FSS proposed some time ago to allow for violation of hyperscaling due to a dangerous irrelevant variable applies only to $\mathbf{k} = \mathbf{0}$ fluctuations, and “standard” FSS applies to $\mathbf{k} \neq \mathbf{0}$ fluctuations. Hence the exponent η describing power-law decay of correlations at criticality is unambiguously $\eta = 0$. With free boundary conditions, the finite-size “shift” is greater than the rounding. Nonetheless, using $T - T_L$, where T_L is the finite-size pseudocritical temperature, rather than $T - T_c$, as the scaling variable, the data do collapse onto a scaling form that includes the behavior both at T_L , where the susceptibility χ diverges like $L^{d/2}$, and at the bulk T_c , where it diverges like L^2 . These claims are supported by large-scale simulations on the five-dimensional Ising model.

DOI: [10.1103/PhysRevE.90.062137](https://doi.org/10.1103/PhysRevE.90.062137)

PACS number(s): 05.50.+q, 05.70.Jk, 64.60.an, 64.60.F–

I. INTRODUCTION

The method of finite-size scaling (FSS) [1–3] has been successfully applied to the analysis of the results of many numerical simulations. The main ingredient is the assumption that finite-size corrections only involve the ratio of the system size L to the bulk (i.e., infinite system size) correlation length ξ . The latter diverges as T approaches the transition temperature T_c like $\xi \propto (T - T_c)^{-\nu}$, where ν is the correlation length exponent.

While this assumption is undoubtedly correct in dimensions below the upper critical dimension d_u , equal to 4 for most systems, the situation is, surprisingly, more complicated for $d > d_u$, even though the critical exponents are given by their mean-field values in this region. The reason is that a “dangerous irrelevant” variable, see, e.g., Appendix D in [4], causes scaling functions to have additional singularities. While the nature of FSS above the upper critical dimension has been clarified for $\mathbf{k} = \mathbf{0}$ fluctuations in systems with periodic boundary conditions, the situation in models with free boundary conditions, and for $\mathbf{k} \neq \mathbf{0}$ fluctuations for both boundary conditions, seems confused. The purpose of the work presented here is to clarify these questions and to present a simple, unified picture of FSS above the upper critical dimension.

According to *standard* FSS, valid for $d < d_u$, a susceptibility χ that diverges in the bulk like $(T - T_c)^{-\gamma}$ for $T \rightarrow T_c$ has a FSS form

$$\chi(L, T) = L^{\gamma_T} \bar{X}[L^{\gamma_T} (T - T_c)], \quad (1)$$

where γ_T is the thermal exponent in the renormalization-group sense and is related to the correlation length exponent by

$$\gamma_T = 1/\nu. \quad (2)$$

The argument of the scaling function \bar{X} is proportional to $(L/\xi)^{1/\nu}$, so Eq. (1) implements the basic FSS assumption, stated above, that finite-size effects depend on the ratio L/ξ [5]. Above T_c and for large L , finite-size effects disappear, so we must recover the bulk result, which requires $\bar{X}(x) \propto x^{-\gamma}$ for $x \rightarrow \infty$.

Finite-size scaling is particularly simple for dimensionless (more generally scale-invariant) quantities for which the exponent γ above is zero. An example is the dimensionless ratio of the moments of the order parameter proposed by Binder [6]. The Binder ratio, g , defined in Eq. (22) below, has the standard FSS form

$$g(L, T) = \bar{g}[L^{\gamma_T} (T - T_c)]. \quad (3)$$

One sees that the data are independent of size at T_c , so data for different sizes intersect there, which provides a very convenient way of locating T_c . Furthermore, the scaling functions $\bar{X}(x)$ and $\bar{g}(x)$ are predicted to be universal [apart from a nonuniversal metric factor multiplying the argument x , and a nonuniversal factor multiplying the prefactor L^{γ_T} in Eq. (1)], so the value of g at T_c is predicted to be universal.

The purpose of the present work is to discuss how Eqs. (1) and (3) are modified for $d > d_u = 4$. First of all we note that, in this region, we have mean-field exponents whose values are $\gamma = 1, \gamma_T = 1/\nu = 2$, so naively we would have

$$\chi(L, T) = L^2 \bar{X}[L^2 (T - T_c)], \quad (4a)$$

$$g(L, T) = \bar{g}[L^2 (T - T_c)]. \quad (4b)$$

As discussed above, the power 2 in these equations is the value of the thermal exponent $\gamma_T (=1/\nu)$ in the mean-field region. For periodic boundary conditions and, implicitly, for $\mathbf{k} = \mathbf{0}$ fluctuations, Binder *et al.* [7] showed that one should not use the thermal exponent γ_T but rather modify Eq. (4) to

$$\chi(L, T) = L^{\gamma_T^*} \bar{X}[L^{\gamma_T^*} (T - T_c)], \quad (5a)$$

$$g(L, T) = \bar{g}[L^{\gamma_T^*} (T - T_c)] \quad (\text{periodic, } \mathbf{k} = \mathbf{0}), \quad (5b)$$

where

$$\gamma_T^* = d/2. \quad (6)$$

Reference [7] argued that the scaling involves γ_T^* rather than γ_T by requiring that a natural FSS assumption for the free energy gives the correct *bulk* behavior in all limiting cases. Since $d > 4$, we have $\gamma_T^* > \gamma_T (=2)$.

The modification of Eq. (4) to Eq. (5) for finite-size effects is related to the breakdown of hyperscaling for

bulk quantities. Hyperscaling relations are those relations between exponents that involve the dimensionality d such as

$$d\nu = 2 - \alpha, \tag{7}$$

where α is the specific-heat exponent. For $d > d_u = 4$, the exponents stick at their mean-field values $\nu = 1/2, \alpha = 0$ so Eq. (7) is not valid except precisely at the upper critical dimension. Both the modification of Eq. (4) to Eq. (5) and the violation of hyperscaling come from a “dangerous” irrelevant variable [4]. The irrelevant variable, which is the quartic coupling in the field theory formulation, is “dangerous” because scaling functions develop a singularity as it tends to its fixed-point value of zero.

The universal value of \bar{g} at T_c was computed by Brézin and Zinn-Justin [8], who showed it to be simply that obtained by including *only* the $\mathbf{k} = \mathbf{0}$ mode (with T_c adjusted to the correct value). An extensive set of works (see, for example, [3,9–12] and references therein) have shown the validity of Eq. (5), though it required large system sizes, good statistics, and an appreciation that *corrections* to FSS (which occur if the sizes are not big enough) are quite large and slowly decaying, to confirm the predicted, universal value of the Binder ratio at T_c .

Equation (5) is for periodic boundary conditions, so it is interesting to ask what happens for other boundary conditions such as free boundary conditions. Equation (5) is actually rather surprising since it predicts that finite-size corrections appear not when $\xi \sim L$, so $|T - T_c| \sim 1/L^2$, as one would expect, but only when $\xi \sim L^{d/4}$, a larger scale, so $|T - T_c| \sim 1/L^{d/2}$, closer to T_c than expected. However, as noted by Jones and Young [13], surely *something* must happen when $\xi \sim L$ with free boundary conditions, but what? In fact, in an underappreciated paper, Rudnick *et al.* [14] had previously argued *analytically* that a temperature *shift* of order $1/L^2$ has to be included with free boundary conditions, in addition to a rounding of order $1/L^{d/2}$.

Even in the early days of FSS [1,2], the possibility that a “shift” exponent could be different from the “rounding” exponent was allowed for. To explain what this means, note that the exponents 2 in Eq. (4) and $d/2$ in Eq. (5) are “rounding” exponents since they control the range of temperature over which a singularity is rounded out (L^{-2} and $L^{-d/2}$, respectively). To define the “shift” exponent, we first define, for each size, a “finite-size pseudocritical temperature” T_L by, for example, the location of the peak in some susceptibility, or the temperature at which the Binder ratio has a specified value. The difference $T_c - T_L$ goes to zero for $L \rightarrow \infty$ like

$$T_c - T_L = \frac{A}{L^\lambda}, \tag{8}$$

which is the desired definition of the shift exponent λ . The precise value of T_L depends on which criterion is used to define it, but the exponent λ is expected to be independent of the definition. Whether or not the amplitude A depends on the quantity used to define the shift will be discussed in Sec. V. If λ is less than the rounding exponent, which will turn out to be the case for free boundary conditions, then the shift is *larger* than the rounding, so we need to modify

Eq. (5) to

$$\chi(L, T) = L^{y_T^*} \bar{X}[L^{y_T^*} (T - T_L)], \tag{9a}$$

$$g(L, T) = \bar{g}[L^{y_T^*} (T - T_L)] \quad (\text{free, } \mathbf{k} = \mathbf{0}), \tag{9b}$$

in which the argument of the scaling function involves the difference between T and the “finite-size pseudocritical temperature” T_L , and $y_T^* = d/2$; see Eq. (6). We verify Eqs. (9) in Figs. 7, 8, 10, and 12, and in Eqs. (37) and (40) below.

The criterion that the shift is given by the condition $\xi \sim L$ yields $\lambda = 2$, as proposed by Rudnick *et al.* [14] and confirmed in simulations by Berche *et al.* [15,16]. As with Eq. (1), we must have $\bar{X}(x) \propto x^{-1}$ for $x \rightarrow \infty$ in order to recover the bulk behavior above T_c . If we set $T = T_c$, then $L^{d/2} (T - T_L) = AL^{d/2-2}$, which is large so we can use this limiting behavior to get

$$\chi(L, T_c) \propto L^2 \quad (\text{free, } \mathbf{k} = \mathbf{0}), \tag{10}$$

a result that has been shown rigorously [17]. Hence, in contrast to Berche *et al.* [15], we propose that the region at the bulk T_c *is* part of the scaling function. Similarly, for the Binder ratio, $\bar{g}(x) \propto 1/x^2$ for $x \rightarrow \infty$, which gives

$$g(L, T_c) \propto \frac{1}{L^{d-4}} \quad (\text{free, } \mathbf{k} = \mathbf{0}). \tag{11}$$

With periodic boundary conditions, the intersection of the data for g provides a convenient estimate of T_c , but, as Eq. (11) shows, this method cannot be used for free boundary conditions because g vanishes at T_c for $L \rightarrow \infty$. In fact, we shall see from the numerical data in Sec. V that there are no intersections at all. However, we will not be able to verify the precise form in Eq. (11) because the values for g at T_c are so small that the signal is lost in the noise.

So far we have discussed only $\mathbf{k} = \mathbf{0}$ fluctuations. However, it is also necessary to discuss fluctuations at $\mathbf{k} \neq \mathbf{0}$, since we need these to determine the spatial decay of the correlation functions. Of particular importance is the decay of the correlations at T_c , which fall off with distance like $1/r^{d-2+\eta}$, where the mean-field value of the exponent η is zero. In the mean-field regime, the fluctuations of the $\mathbf{k} \neq \mathbf{0}$ modes are Gaussian, so the Binder ratio is always zero. For the wave-vector-dependent susceptibility, we shall argue that standard FSS, Eq. (4), holds for both boundary conditions (BCs), i.e.,

$$\chi(\mathbf{k}, L, T) = L^2 \tilde{X}[L^2(T - T_c), kL] \quad (\text{both BCs, } \mathbf{k} \neq \mathbf{0}), \tag{12}$$

where we have put the explicit k dependence in a natural way as a second argument of the scaling function. We note that Eq. (12) holds for the spherical model [18–20] with periodic boundary conditions [21]. For free boundary conditions, the Fourier modes are not plane waves, see Sec. II, and, by $\mathbf{k} \neq \mathbf{0}$, we really mean modes that are orthogonal to the uniform magnetization and so they do not develop a nonzero expectation value below T_c .

If we fix $T = T_c$ in Eq. (12) and consider $kL \gg 1$, then the size dependence must drop out so $\tilde{X}(0, y) \propto y^{-2}$ and hence

$$\chi(\mathbf{k}, L, T_c) \propto k^{-2} \quad (kL \gg 1). \tag{13}$$

How, then, do correlations fall off in real space at criticality? To fully understand this, we have to consider separately the contribution from the $\mathbf{k} = \mathbf{0}$ mode, as in Bose-Einstein

condensation. If $C(\mathbf{r})$ is the spin-spin correlation function at displacement \mathbf{r} and $\tilde{C}(\mathbf{k})$ is the corresponding k -space correlation, then, as shown in Eq. (13),

$$\tilde{C}(\mathbf{k}) \propto \frac{1}{k^2} \quad (14)$$

for $k \rightarrow 0$. However, for $\mathbf{k} = \mathbf{0}$ we note that $\tilde{C}(\mathbf{k} = \mathbf{0}) = \chi(L, T)/L^d$, see Eq. (21) below, and from Eq. (5a) this gives

$$\tilde{C}(\mathbf{k} = \mathbf{0}) \propto \frac{1}{L^{d/2}}. \quad (15)$$

The real-space correlation function at distance $L/2$ is then given by the Fourier transform (FT)

$$C(\hat{\mathbf{z}}L/2) = \left(\frac{L}{2\pi}\right)^d \int_{\mathbf{k} \neq \mathbf{0}} \tilde{C}(\mathbf{k}) \exp[i\mathbf{k} \cdot L\hat{\mathbf{z}}/2] d^d k \quad (16)$$

$$+ \tilde{C}(\mathbf{k} = \mathbf{0}). \quad (17)$$

Using Eq. (14), which correctly gives the FT at large r , the first term in Eq. (17) is proportional, on dimensional grounds, to $1/L^{d-2}$. This is smaller than the second term, which is proportional to $1/L^{d/2}$. Hence, $C(\hat{\mathbf{z}}L/2) \propto 1/L^{d/2}$, in agreement with Fig. 1 of Ref. [22]. Nonetheless, correlations fall off with distance like $1/r^{d-2}$. The resolution of this apparent discrepancy is that the $\mathbf{k} = \mathbf{0}$ mode has to be treated separately and gives the dominant contribution to $C(\hat{\mathbf{z}}L/2)$. We therefore do not see the need for the second η -like exponent proposed in Ref. [22].

While Eq. (12) does not seem to have been stated in the literature before, to our knowledge, it is actually quite natural. The dangerous irrelevant variable, which is the quartic coupling in the Ginzburg-Landau-Wilson effective Hamiltonian, is needed to control the expectation value of the ($\mathbf{k} = \mathbf{0}$) order parameter, which leads to nonstandard FSS for $\mathbf{k} = \mathbf{0}$ fluctuations. However, $\mathbf{k} \neq \mathbf{0}$ fluctuations (more precisely, fluctuations that do not acquire a nonzero expectation value) are not directly affected by the dangerous irrelevant variable, and consequently they have standard FSS.

The plan of this paper is as follows. In Sec. II, we define the model to be simulated and the quantities we calculate. To incorporate *corrections* to FSS, we use the quotient method, which is described in Sec. III. The numerical results for periodic boundary conditions are presented in Sec. IV, while those for free boundary conditions are in Sec. V. We briefly summarize our conclusions in Sec. VI.

II. MODEL

We consider an Ising model in $d = 5$ dimensions with Hamiltonian

$$\mathcal{H} = - \sum_{\langle i,j \rangle} J_{ij} S_i S_j, \quad (18)$$

where $J_{i,j} = 1$ if i and j are nearest neighbors and zero otherwise, and the spins S_i take values ± 1 . The number of spins is $N = L^5$ and we perform simulations with periodic and free boundary conditions. Previous simulations have determined the transition temperature very precisely, finding [12]

$$T_c = 8.77846(3). \quad (19)$$

We simulate this model very efficiently using the Wolff [23] cluster algorithm, with which we can study sizes up to $L = 36$ (which has around 60 million spins).

We calculate various moments of the uniform magnetization per spin,

$$m = \frac{1}{L^d} \sum_{i=1}^N S_i, \quad (20)$$

as well as the uniform susceptibility [24]

$$\chi = L^d \langle m^2 \rangle \quad (21)$$

and the Binder ratio

$$g = \frac{1}{2} \left(3 - \frac{\langle m^4 \rangle}{\langle m^2 \rangle^2} \right). \quad (22)$$

In addition, we compute the Fourier transformed susceptibilities

$$\chi(\mathbf{k}) = L^d \langle |m(\mathbf{k})|^2 \rangle, \quad (23)$$

in which the Fourier transformed magnetization, $m(\mathbf{k})$, is defined differently for periodic and free boundary conditions as follows.

For periodic boundary conditions, the Fourier modes are plane waves, so we have

$$m(\mathbf{k}) = \frac{1}{N} \sum_i e^{i\mathbf{k} \cdot \mathbf{r}_i} S_i \quad (\text{periodic}), \quad (24)$$

where

$$k_\alpha = 2\pi n_\alpha / L \quad (\text{periodic}), \quad (25)$$

with $n_\alpha = 0, 1, \dots, L-1$, and α denotes a Cartesian coordinate.

For free boundary conditions, the Fourier modes are sine waves,

$$m(\mathbf{k}) = \frac{1}{N} \sum_i \left[\prod_{\alpha=1}^d \sin(k_\alpha r_{i,\alpha}) \right] S_i \quad (\text{free}), \quad (26)$$

where

$$k_\alpha = \pi n_\alpha / (L+1) \quad (\text{free}), \quad (27)$$

with $n_\alpha = 1, 2, \dots, L$ and the components of the lattice position, $r_{i,\alpha}$, also run over values $1, 2, \dots, L$. There is zero contribution to the sum in Eq. (26) if we set $r_{i,\alpha} = 0$ or $L+1$, so Eqs. (26) and (27) correctly incorporate free boundary conditions.

Note that $\mathbf{k} = \mathbf{0}$ is not an allowed wave vector with free boundary conditions, so the uniform magnetization in Eq. (20) does not correspond to a single Fourier mode. Note, too, that wave vectors with all n_α odd have a projection onto the uniform magnetization and so will acquire a nonzero expectation value below T_c in the thermodynamic limit. They will therefore be subject to the nonstandard FSS in Eq. (5). However, if any of the n_α are even, there is no projection onto the uniform magnetization, so they will not acquire an expectation value below T_c and will therefore be subject to the standard FSS in Eq. (12).

III. THE QUOTIENT METHOD

The discussion in Sec. I assumed that the sizes are sufficiently large and T sufficiently close to T_c that corrections to FSS are negligible. For free boundary conditions, however, a substantial fraction of the spins lies on the surface, so *corrections* to FSS are quite large and need to be included in the analysis. In this section, we describe the method we used to include the *leading* correction to FSS.

A convenient way to extract the leading scaling behavior from the data, in the presence of corrections, is the quotient method [26], which is based on Nightingale’s [27] phenomenological scaling. As an example, consider the deviation of the pseudocritical temperature T_L from T_c for which the FSS expression is given in Eq. (8). Including the leading correction to scaling, which involves a universal exponent ω , one has

$$\Delta T(L) \equiv T_c - T_L = \frac{A}{L^\lambda} \left(1 + \frac{B}{L^\omega} \right). \quad (28)$$

We determine the quotient $Q[\Delta T]$ by taking the log of the ratio of the result for sizes L and sL , where s is a simple rational fraction like 2 or 3/2, and we divide by $\ln s$, i.e.,

$$Q_{s,L}[\Delta T] = \frac{1}{\ln s} \ln \left(\frac{\Delta T(sL)}{\Delta T(L)} \right). \quad (29)$$

According to Eq. (28) we have, for large L ,

$$Q_{s,L}[\Delta T] = -\lambda + \frac{C_s}{L^\omega}, \quad (30)$$

where

$$C_s = \frac{s^{-\omega} - 1}{\ln s} B. \quad (31)$$

If the data are of sufficient quality, we can fit all the unknown parameters. In Eq. (30), these would be λ , ω , and C_s . In most cases, however, we will need to assume the predicted value for the correction exponent ω , see below, and just fit to the other parameters.

According to the renormalization group, for $d > d_u = 4$, the leading irrelevant variable has scaling dimension

$$\omega = d - 4. \quad (32)$$

However, for $\mathbf{k} = \mathbf{0}$ fluctuations and periodic boundary conditions, it was shown in Ref. [8] that there is an additional, and larger, correction for finite-size effects, with an exponent given by

$$\omega' = \frac{d - 4}{2}. \quad (33)$$

An intuitive way to see this is to note that the “naive” variation of χ with L at the critical point, $\chi \propto L^2$ [see Eq. (4a)], although not the dominant contribution [which is $L^{d/2}$ as shown in Eq. (5a)], is nonetheless still present as a correction. This correction is down by a factor of $L^{2-d/2}$ ($=L^{-\omega'}$) relative to the dominant term. We shall therefore use ω' rather than ω in considering corrections to scaling for susceptibilities that scale with L to the power $d/2$ rather than 2.

For some of our data, we will also need subleading corrections to FSS for which there are several contributions. One of these is the square of the leading contribution. To avoid having too many fit parameters, this is the form we

shall assume, i.e., when we include subleading corrections to scaling we will do a parabolic fit in $1/L^\omega$ (or $1/L^{\omega'}$ as the case may be).

A subtlety arises in doing fits to data for quotients, for example to determine the parameters λ , ω , and C_s in Eq. (30). The reason is that the same set of simulational data may be used in the determination of more than one data point in the fit. For example, with $s = 2$ the $L = 16$ simulation data are incorporated into the pairs (8,16) and (16,32). Furthermore, we will do combined fits incorporating data for two different values of s ($s = 2$ and $3/2$), using the *same* exponents (since they are universal), but with different amplitudes (because they are not universal). This has the advantage of increasing the number of data points in the fit by more than the number of parameters. Again, the same set of simulational data is used to determine different data points in the fit. Hence the different quotient values being fitted are *not statistically independent*. The best estimate of the fitting parameters should include these correlations [26,28,29]. In other words, if a data point is (x_i, y_i) and the fitting function is $u(x)$, which depends on certain fitting parameters, those parameters should be determined by minimizing

$$\chi^2 = \sum_{i,j} [y_i - u(x_i)](C^{-1})_{ij}[y_j - u(x_j)], \quad (34)$$

where

$$C_{ij} = \langle y_i y_j \rangle - \langle y_i \rangle \langle y_j \rangle \quad (35)$$

is the covariance matrix of the data. We determine the elements of the covariance matrix by a bootstrap analysis [30,31]. If there are substantial correlations in many elements, the covariance matrix can become singular, and where this happened we projected onto the eigenvectors of the covariance matrix whose eigenvalues are not (close to) zero, ignoring eigenvectors corresponding to zero eigenvalues. The effective number of independent data points is then the rank of the covariance matrix (the number of nonzero eigenvalues).

IV. RESULTS: PERIODIC BOUNDARY CONDITIONS

A. $k = 0$ fluctuations

We shall be brief here, since there is no dispute that the FSS scaling in Eq. (5) is correct, but we will show some results for completeness.

The left-hand panel of Fig. 1 presents an overview of our data for the Binder ratio g , showing intersections at, or close to, the transition temperature T_c given in Eq. (19). The expanded view in the middle panel shows that the intersections for different pairs of sizes do not occur at exactly the same value, indicating corrections to scaling. In fact, the data for smaller sizes have an approximate intersection at a value larger than the exact, universal value of [8]

$$g_c = \frac{1}{2} \left(3 - \frac{\Gamma^4(\frac{1}{4})}{8\pi^2} \right) = 0.40578. \quad (36)$$

However, for larger sizes the intersections occur at smaller values of g . The right-hand panel of Fig. 1 shows an additional set of data taken at precisely $T = T_c$, plotted against $L^{-\omega'}$ with the correction exponent given by $\omega' = 1/2$; see the discussion

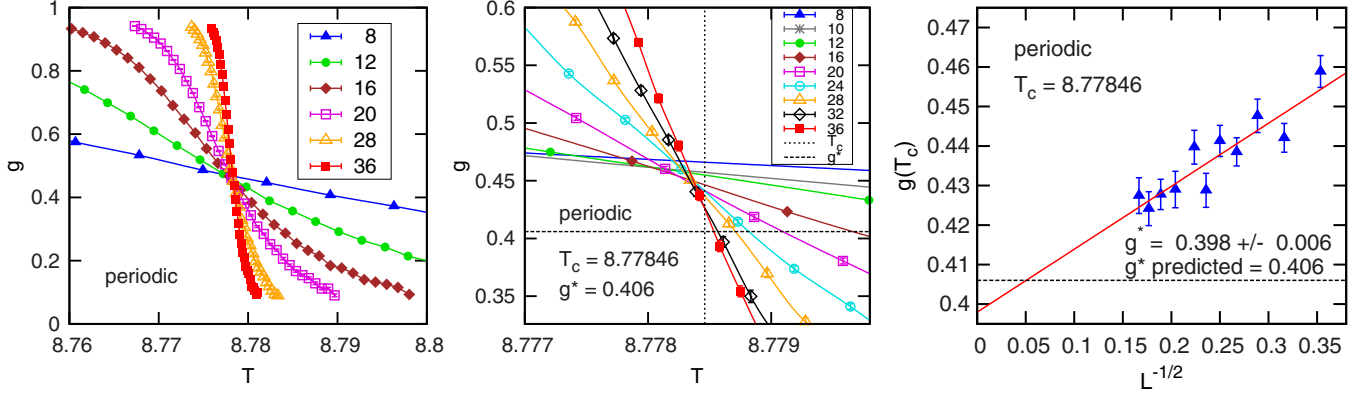


FIG. 1. (Color online) The left panel shows an overview of our results for the Binder ratio g for periodic boundary conditions. In the middle panel, which shows an expanded view near T_c , the dashed vertical line indicates T_c given by Eq. (19), and the dashed horizontal line indicates the universal value for g_c given by Eq. (36). The right panel shows an additional set of results for g taken precisely at T_c , plotted against $L^{-\omega'}$ with $\omega' = 1/2$, see Eq. (33), and a straight-line fit indicating an extrapolated value for $L \rightarrow \infty$ consistent with (1.3 σ difference) the exact result. The quality-of-fit factor [25] is $Q = 0.252$.

in Sec. III. The data decrease to a value consistent with Eq. (36) for $L \rightarrow \infty$. As noted by other authors, the effect of a fairly slow correction to a scaling exponent, $\omega = 1/2$, combined, evidently, with a fairly large correction amplitude, has made it very difficult to obtain the known exact result for g_c from numerics. This should serve as a cautionary tale when applying FSS to other problems where the exact answer is not known.

B. $k \neq 0$ fluctuations

The data for $\chi(\mathbf{k})$ for $\mathbf{k}L/(2\pi) = (1,0,0,0)$ are shown in Fig. 2. Note that the Fourier components at nonzero wave vector do not develop order below T_c , and so what we define as $\chi(\mathbf{k})$ really is the susceptibility below T_c as well as above it (unlike the $\mathbf{k} = 0$ susceptibility [24]), and consequently the

data have a peak, whereas the uniform “susceptibility” plotted in Fig. 9 below (for free boundary conditions) continues to increase below T_c .

A scaling plot of the data is shown in Fig. 3 according to the standard FSS in Eq. (12). Apart from the smallest size, $L = 8$, near T_c the data scale very well. Going further away from T_c on the low- T side, we see bigger corrections. However, this is unsurprising since FSS is only expected to work for T close to T_c .

If we go to larger k values, we get a similar picture but with bigger corrections to scaling, as shown in Fig. 4 for $\mathbf{k}L/(2\pi) = (1,1,0,0)$. It is expected that corrections to scaling become *relatively* bigger for larger k because the signal is less divergent in this case, and so it is more easily affected by corrections.

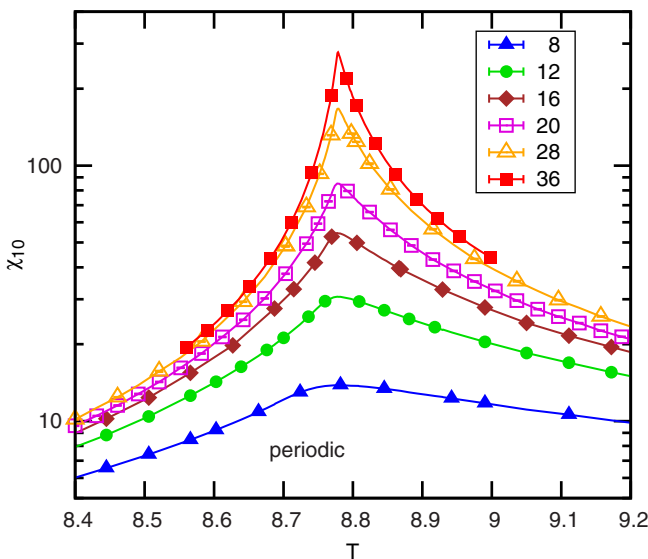


FIG. 2. (Color online) Susceptibility of $\chi(\mathbf{k})$ for $\mathbf{k}L/(2\pi) = (1,0,0,0)$, which we abbreviate to χ_{10} , for periodic boundary conditions. For clarity, only a representative selection of data points is shown, but the lines go through all the points.

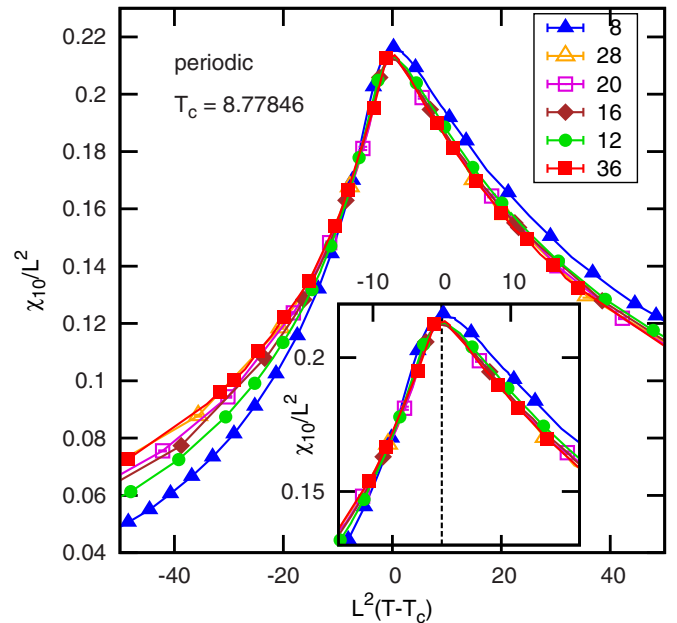


FIG. 3. (Color online) A scaling plot of the susceptibility of the data in Fig. 2. The inset shows an enlarged view near T_c . The horizontal axis is $L^2(T - T_c)$ for both plots.

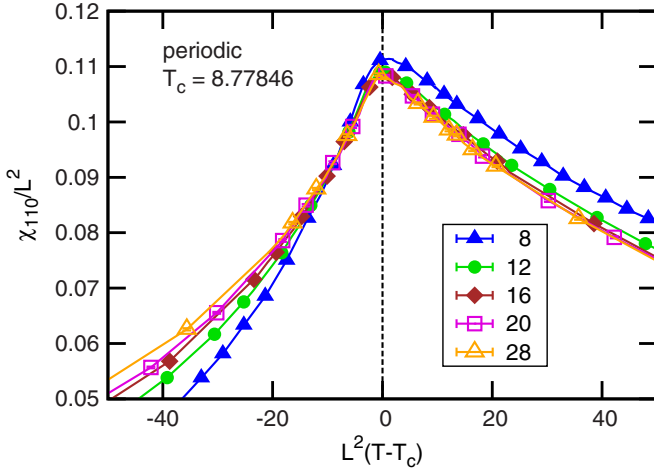


FIG. 4. (Color online) A scaling plot of the susceptibility $\chi(\mathbf{k})$ for $\mathbf{k}L/(2\pi) = (1, 1, 0, 0, 0)$, which we abbreviate to χ_{110} , for periodic boundary conditions.

Figure 5 shows the behavior of $\chi(\mathbf{k})/L^2$ at T_c showing that it is a function of the product kL as expected; see Eq. (12). The dashed line has slope -2 indicating that the expected k^{-2} behavior in Eq. (13) sets in even for small values of kL .

V. RESULTS: FREE BOUNDARY CONDITIONS

Since corrections to scaling are larger for free boundary conditions than for periodic boundary conditions, in this section we shall make extensive use of the quotient method described in Sec. III to incorporate the leading correction.

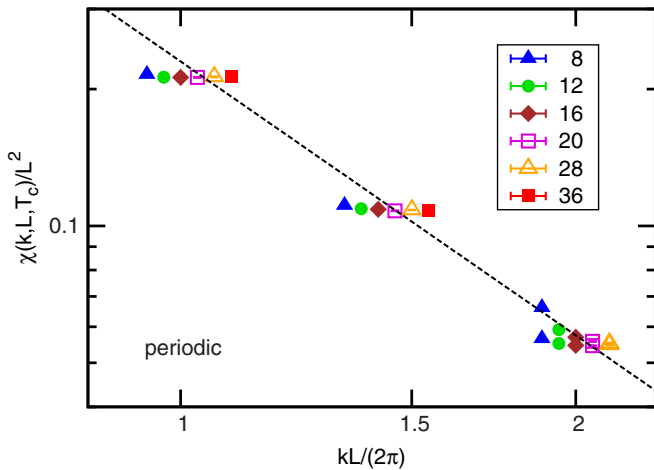


FIG. 5. (Color online) The values of $\chi(\mathbf{k})/L^2$ at T_c for periodic boundary conditions. The points for different sizes and a single value of the x coordinate are displaced slightly horizontally, so they can be distinguished. Data are shown for three different values of the x coordinate: $1, \sqrt{2}$, and 2 . There are actually two different wave vectors for $kL/(2\pi) = 2$, namely those with $\mathbf{k}L/(2\pi) = (2, 0, 0, 0, 0)$ and $(1, 1, 1, 1, 0)$. These two agree well except for the smaller sizes, showing that the fluctuations are isotropic at long wavelength. The dashed line has a slope -2 , indicating that the expected k^{-2} behavior in Eq. (13) sets in even for small values of kL .

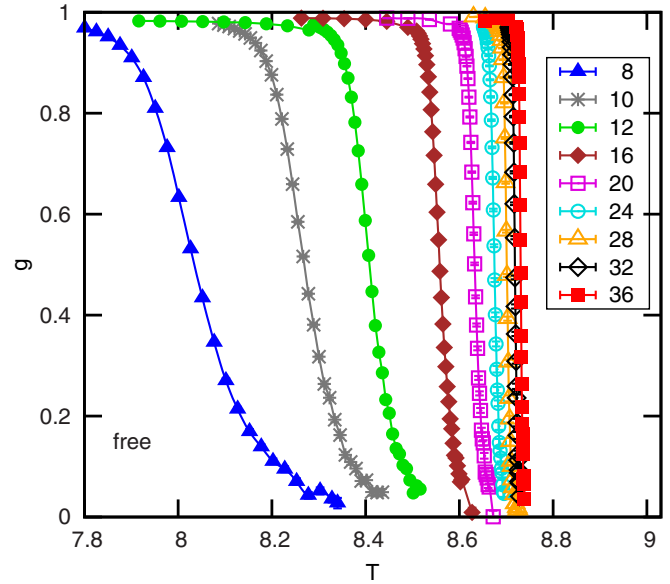


FIG. 6. (Color online) An overview of our results for the Binder ratio g for free boundary conditions. Note that there is no sign of any intersections, and there is a large shift to lower temperatures for the smaller sizes.

A. $k = 0$ fluctuations

An overview of our results for the Binder ratio is shown in Fig. 6. We do not find any intersections, and the data are shifted considerably to lower temperatures for smaller sizes.

To determine the shift exponent, we define the pseudo-critical temperature T_L to be where g takes the value $1/2$, halfway between its limiting values of 0 and 1 . We subtract T_c given in Eq. (19) and determine the resulting quotients for $\Delta T(L) \equiv T_c - T_L$ according to Eq. (29). These quotients are then fitted according to Eq. (30), as shown in Fig. 7. The quality of the data is very good, the signal to noise is high, and we are able to fit all three parameters λ, ω , and the amplitude C . The

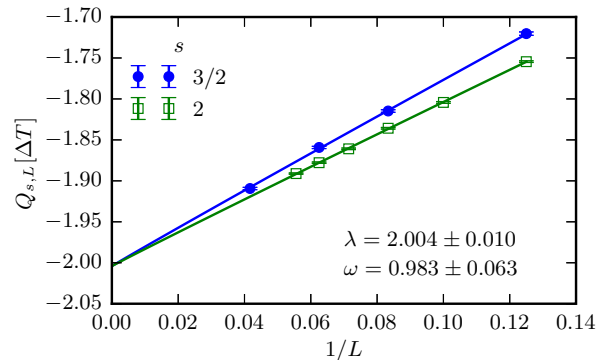


FIG. 7. (Color online) Quotients for $\Delta T(L)$, defined in Eq. (28), used to determine the shift exponent λ for free boundary conditions. The data are fitted to Eq. (30), and the fitting parameters are λ, ω (the same for both values of s) and separate amplitudes C_2 and $C_{3/2}$. The quality of the linear fit is very good, $Q = 0.42$.

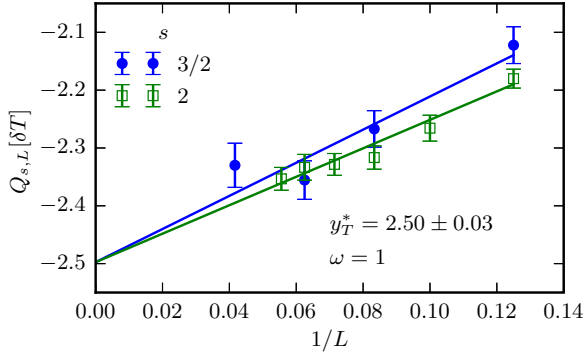


FIG. 8. (Color online) Quotients for $\delta T(L)$ defined in Eq. (38), used to determine the width exponent y_T^* for free boundary conditions. The parameter s is the ratio of two sizes, as shown in Eqs. (29)–(31). The data are fitted to Eq. (39), with fitting parameters y_T^* , A_2 , and $A_{3/2}$. The correction exponent ω is fixed to its expected value of 1. The quality of the straight-line fit is good; $Q = 0.50$.

results for the exponents are

$$\lambda = 2.004(10), \quad \omega = 0.98(6). \quad (37)$$

This value for the shift exponent is in precise agreement with the value $\lambda = 2$ proposed analytically in Ref. [14] and found numerically in Ref. [15]. There is also excellent agreement between our value of the correction to scaling exponent ω and the renormalization group value of 1.

We estimate the rounding by the range in temperature $\delta T(L)$ in which g varies between 0.25 and 0.75, i.e.,

$$\delta T(L) = T(g = 0.25) - T(g = 0.75). \quad (38)$$

Constructing the quotients and fitting to

$$Q_{s,L}[\delta T] = -y_T^* + A_s/L^\omega, \quad (39)$$

we find that the data are insufficient to determine the three parameters, but if we assume the RG value for the correction exponent, $\omega = 1$, then we get a good fit that extrapolates to

$$y_T^* = 2.50(3), \quad (40)$$

see Fig. 8, in precise agreement with the prediction $d/2$, see Eq. (6). We should mention that the quoted error bar *assumes* that the data can be described by Eq. (40); in other words, *subleading* corrections do not affect the fitted data significantly. If this is the case, we have established the values of the shift and rounding exponents in Eq. (9b).

What about the scaling of χ in Eq. (9a)? The data for χ are shown in Fig. 9. We evaluated this at T_L , and we did a quotient analysis, which is shown in Fig. 10. The data are insufficient to determine the correction to the scaling exponent, so we fixed it to the expected value $\omega' = 1/2$. The amplitude of the correction term is large, but the data extrapolate to a value 2.56(4), very close to the value of $y_T^* = 5/2$ expected from Eq. (9a), and which was found in earlier simulations by Berche *et al.* [15,16].

We can also evaluate χ at the bulk T_c . As shown in Eq. (10), this is proportional to L^2 , not $L^{d/2}$, and so, as discussed in Sec. III, we expect that the correction to the scaling exponent will be $\omega (=1)$ rather than $\omega' (=1/2)$. Quotients of the results are plotted in Fig. 11. There are clearly subleading

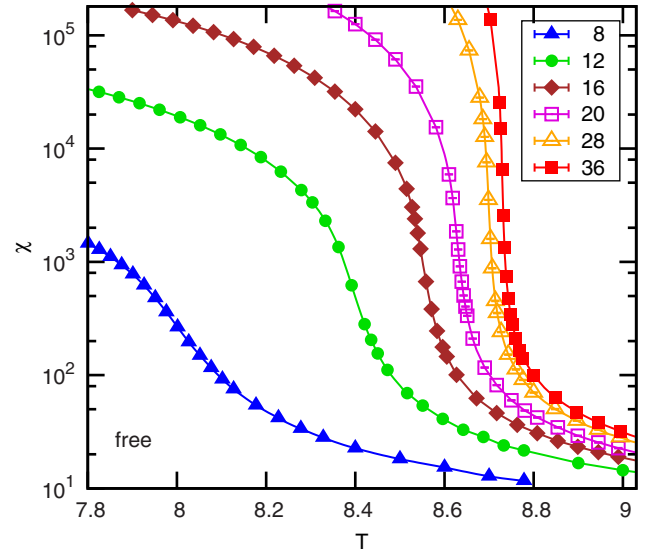


FIG. 9. (Color online) Data for χ for free boundary conditions. Only a representative set of points are shown, but the lines go through all the points. Note that with the definition in Eq. (21), a term proportional to the square of the order parameter is not subtracted off, so χ as defined is really only the susceptibility above T_c , and it continues to rise below T_c .

corrections to scaling, so we try a quadratic fit, with the result $y_T = 1.97(6)$, in good agreement with the expected value of 2. We note that corrections to scaling are quite large, which is not surprising since the values of χ at T_c are quite small, and so they are more influenced by several corrections to scaling than the data at T_L , which χ is bigger. We also tried a linear fit omitting the smallest size for each value of s finding 1.89(2) with $Q = 0.30$, which differs by more than the error bar from the value 2. Nonetheless, the quadratic fit shows that, although we have not determined the exponent with which χ diverges at T_c with great accuracy, it is, at the very least, *consistent* with the

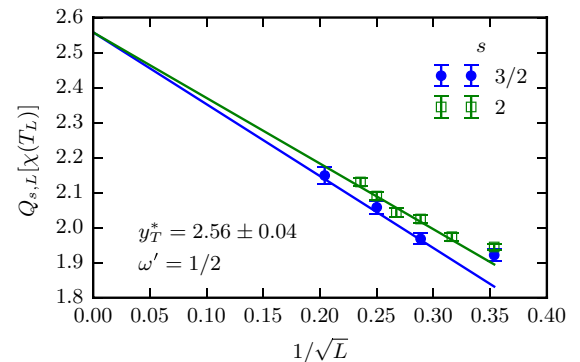


FIG. 10. (Color online) Quotients for the value of χ at T_L for free boundary conditions plotted against $1/L^{\omega'}$, where the correction to the scaling exponent ω' is fixed to the value 1/2. According to Eq. (9a), the quotients should extrapolate to a value of $y_T^* (=5/2)$ for $L \rightarrow \infty$. The linear fit omits the right-hand point for each of the data sets, and the three fitting parameters are the value of y_T^* and two amplitudes of the correction, one for each value of s . The quality of the fit is good, $Q = 0.30$.

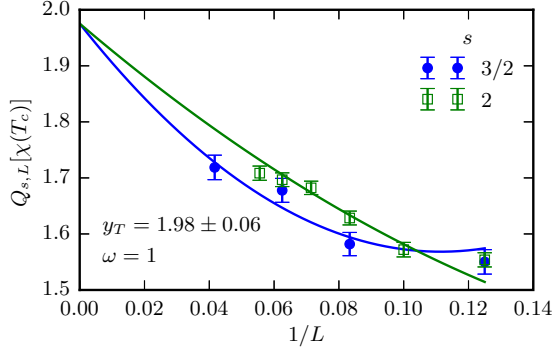


FIG. 11. (Color online) A quadratic fit for the quotients for value of χ at the bulk T_c for free boundary conditions against $1/L^\omega$ where the correction to the scaling exponent ω is fixed to the value 1. According to Eq. (10), the quotients should extrapolate to the value of y_T ($=2$). There are five fitting parameters: y_T and the amplitudes of the linear and quadratic corrections for each s value. The quality of the fit is good, $Q = 0.43$.

value of 2 expected according to Eq. (10). An L^2 divergence of the susceptibility at the bulk transition temperature has also been found recently [32] in work that was able to study larger sizes than the values we studied, up to $L = 160$.

Figure 12 shows a scaling plot of $\chi(T)/\chi(T_L)$ against $L^{d/2}(T - T_L)/T_L$. We have seen in Fig. 10 that there are corrections to the expected $L^{d/2}$ behavior of χ at T_L for the range of sizes studied. Hence we divide $\chi(T)$ by $\chi(T_L)$ rather than by $L^{d/2}$, which appears in Eq. (9a), to eliminate those corrections to scaling in Fig. 12. According to Eq. (9a), the data in Fig. 12 should collapse. There are some corrections to this, which is not surprising since we are probing the scaling function over a big region, but overall the data scale pretty well. Also shown are data at T_c , which appear at different points for

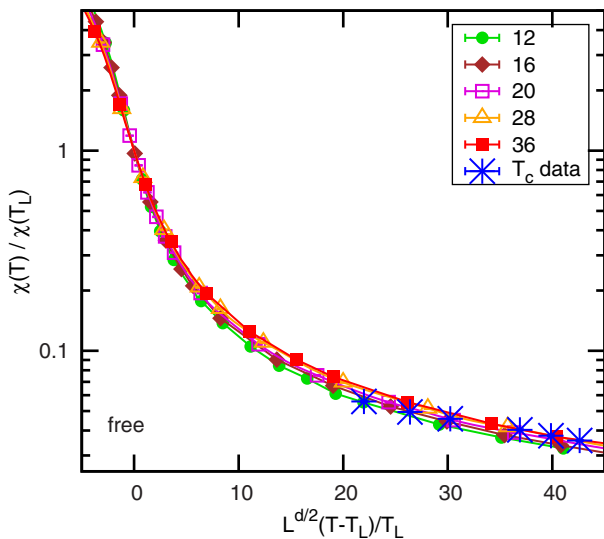


FIG. 12. (Color online) A scaling plot of the data for χ for free boundary conditions according to Eq. (9a). Also shown are the data at T_c , which are seen to lie on the scaling function (within some small corrections).

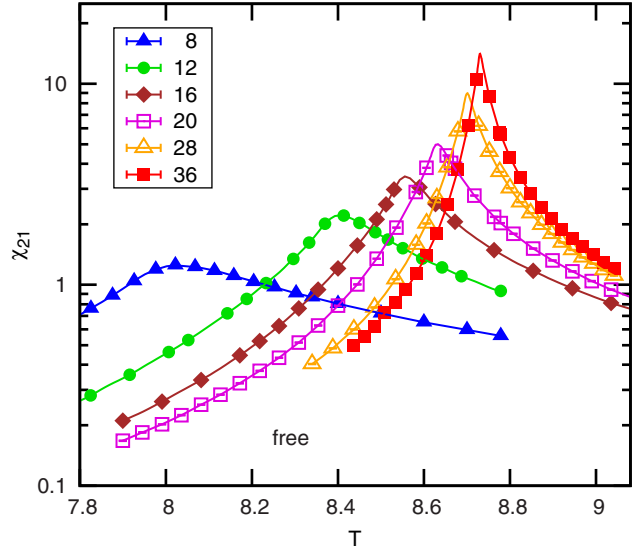


FIG. 13. (Color online) Data for $\chi(\mathbf{k})$ for $(L + 1)\mathbf{k}/\pi = (2, 1, 1, 1)$ for free boundary conditions. Only a representative set of points are shown, but the lines go through all the points.

different sizes because T_L is, of course, size-dependent. The larger the size, the further to the right is the data point for T_c . This figure supports our claim that the data at T_c are included in the scaling function in Eq. (9a).

We have defined the pseudocritical temperatures T_L and the resulting shift exponent λ , from Eq. (8), by the temperature where the Binder ratio takes the value $1/2$. Suppose we took a different criterion for T_L , such as the temperature at which the Binder ratio has some other value, or where there is a peak in some $\mathbf{k} \neq \mathbf{0}$ susceptibility such as that shown in Fig. 13. We note that the finite-size width varies as $1/L^{d/2}$, so temperatures at which the Binder ratio has a value between 0 and 1 would lie in this range, and so they would only give a *subleading* contribution to the shift, the coefficient of $1/L^2$ remaining the same. We expect that the same shift amplitude would be obtained no matter what quantity is used to define the shift for the following reason. Suppose we have a shift amplitude A and pseudocritical temperatures T_L determined from where the Binder ratio is $1/2$ and a different amplitude A' , and correspondingly different temperatures T'_L , determined by some other criteria. Then the Binder ratio has a scaling form in Eq. (9b), but if we try to define it in terms of the alternative shift temperatures T'_L , we have

$$g(L, T) = \bar{g}[L^{d/2}(T - T_L)] \tag{41}$$

$$= \bar{g}[L^{d/2}(T - T'_L) + (A' - A)L^{d/2-2}]. \tag{42}$$

Hence, if different quantities give different shift amplitudes, the argument of the scaling function would be shifted by an *infinite* amount (for $L \rightarrow \infty$) if we use the shift obtained from a different quantity. This would be a clear violation of scaling. We postulate that this does not happen and that there is a *unique* shift amplitude for a given system.

Note, however, that we cannot rule out subleading corrections to the shift of order $1/L^{d/2}$. As a result, the value of g at

T_L according to Eq. (9b) will depend on the precise definition of T_L and therefore will *not* be universal, unlike the situation with periodic boundary conditions; see Eq. (5b). Hence one can view the replacement of Eqs. (5) by Eqs. (9) as a violation of standard finite-size scaling [14]. However, since the behavior of χ , for example, is described by a single function both at T_c and T_L , we view Eqs. (9) as representing a *modified FSS*, distinct from standard FSS, in that it has different shift and scaling exponents.

B. $k \neq 0$ fluctuations

With free boundary conditions, the Fourier modes are sine waves given by Eq. (27). Modes in which all the integers n_α are odd have a projection on the uniform magnetization and so will therefore have a nonzero magnetization. These will therefore be affected by the dangerous irrelevant variable, and so have the same scaling as fluctuations of the uniform magnetization, given in Eq. (9a). We therefore take the smallest wave vector with an even n_α , namely $\mathbf{n} = (2, 1, 1, 1)$, since this will not acquire a nonzero magnetization, so we expect it to be governed by the FSS in Eq. (12), i.e., with exponent 2 rather than $d/2$, which appears in Eq. (9a). We show the data in Fig. 13.

According to Eq. (12), the height of the peaks in Fig. 13 should scale as L^2 and the width should scale as L^{-2} . We define the width to be the difference between the two temperatures where the susceptibility is $3/4$ of that at the maximum. The quotient analyses for height and width are shown in Figs. 14 and 15, respectively. For the height, the (quadratic) fit gives an extrapolated value of $2.010(24)$, which agrees with the expected value of $y_T = 2$. As discussed in the caption to Fig. 14, a linear fit gave a value $1.950(2)$, close to but slightly different from 2. However, the quality of fit factor $Q = 0.002$ [25] was unacceptably low, which is why we went to a quadratic fit. For the data of the width in Fig. 15, the dependence on size is modest and we find an

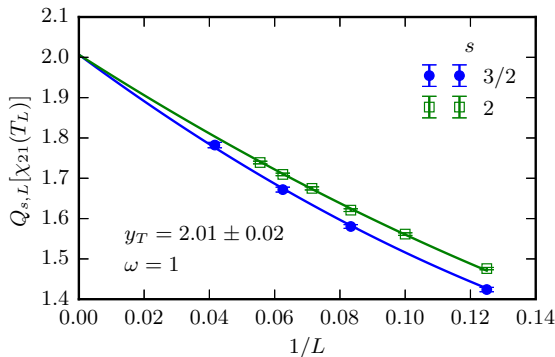


FIG. 14. (Color online) Quotients for the value of $\chi(\mathbf{k})$ for $(L+1)\mathbf{k}/\pi = (2, 1, 1, 1)$ at T_L for free boundary conditions. The correction to the scaling exponent of $\omega = 1$ is taken. According to Eq. (12), the quotients should tend to the value $y_T (=2)$ for $L \rightarrow \infty$. As in other quotient fits, we use the same values for the exponents y_T and ω for the two values of s , but different amplitudes for the corrections to scaling. Here we use a quadratic fit that worked well, $Q = 0.53$. A linear fit gave an extrapolated value of $1.950(2)$ but with a poor quality of fit factor $Q = 0.002$.

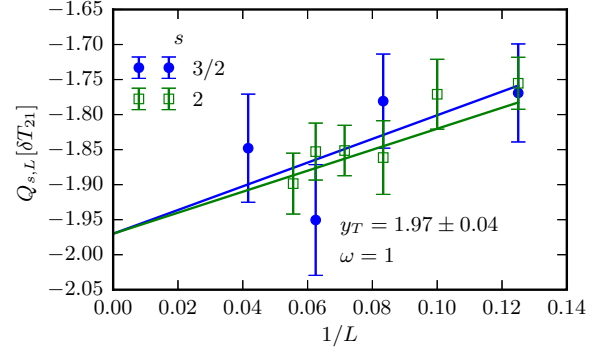


FIG. 15. (Color online) A linear fit to quotients for the width of the peak in $\chi(\mathbf{k})$ for $(L+1)\mathbf{k}/\pi = (2, 1, 1, 1)$ for free boundary conditions. The correction to the scaling exponent of $\omega = 1$ is taken. According to Eq. (12), the quotients should tend to $-y_T (= -2)$ for $L \rightarrow \infty$. The amplitude of the correction to scaling is seen to be quite small in this case, and the quality of the linear fit is excellent: $Q = 0.67$.

extrapolated value of $-1.97(4)$ consistent with the expected value of $-y_T (= -2)$.

Consequently, we have found strong evidence to support our claim that Eq. (12) applies to free boundary conditions. Note that since this FSS scaling form uses $y_T (=2)$ and the deviation of T_L from T_c is proportional to $1/L^2$, asymptotically we can use either T_c or T_L in Eq. (12).

VI. SUMMARY AND CONCLUSIONS

Our main conclusions have already been discussed in the Introduction, so we will be brief here. FSS above the upper critical dimension can be summarized as follows:

(i) The modified FSS form with exponents $d/2$ rather than 2 only applies to $\mathbf{k} = \mathbf{0}$ fluctuations. (For free boundaries, it applies to Fourier modes that have a projection onto the uniform magnetization.) For all other wave vectors, standard FSS with an exponent 2 applies. As a result, there the exponent η describing the power-law decay of correlations at T_c is unambiguously $\eta = 0$. (See Figs. 3–5, 14, and 15.)

(ii) For free boundaries and at $\mathbf{k} = \mathbf{0}$, the shift, with an exponent 2, is larger than the rounding, which has an exponent $d/2$. Using $T - T_L$, where T_L is the finite-size, pseudocritical temperature, rather than $T - T_c$, as a scaling variable, the data have a scaling form that incorporates both the behavior at T_L where $\chi \propto L^{d/2}$, and at the bulk T_c where $\chi \propto L^2$. (See Figs 7, 8, and 10–12.)

ACKNOWLEDGMENTS

We would like to thank Michael Fisher for very helpful comments and criticisms on an earlier version of this manuscript, and Joe Rudnick for useful discussions. This work is supported in part by the National Science Foundation under Grant No. DMR-1207036. We also acknowledge support from a Gutzwiller Fellowship at the Max Planck Institute for the Physics of Complex Systems, Dresden.

- [1] M. E. Fisher, in *Critical Phenomena, Proceedings of the 51st Enrico Fermi Summer School, Varenna*, edited by M. S. Green (Academic, New York, 1971), p. 1.
- [2] M. E. Fisher and M. N. Barber, *Phys. Rev. Lett.* **28**, 1516 (1972).
- [3] K. Binder and E. Luijten, *Phys. Rep.* **344**, 179 (2001).
- [4] M. E. Fisher, in *Advanced Course on Critical Phenomena*, edited by F. W. Hahne (Springer, Berlin, 1983), p. 1.
- [5] It is convenient to take L/ξ to the power $1/\nu$ because then $T - T_c$ appears linearly, with the result that a single scaling function applies both above and below T_c .
- [6] K. Binder, *Phys. Rev. Lett.* **47**, 693 (1981).
- [7] K. Binder, M. Nauenberg, V. Privman, and A. P. Young, *Phys. Rev. B* **31**, 1498 (1985).
- [8] E. Brézin and J. Zinn-Justin, *Nucl. Phys. B* **257**, 867 (1985).
- [9] E. Luijten and H. W. J. Blöte, *Phys. Rev. Lett.* **76**, 1557 (1996).
- [10] G. Parisi and J. J. Ruiz-Lorenzo, *Phys. Rev. B* **54**, R3698 (1996).
- [11] H. W. J. Blöte and E. Luijten, *Europhys. Lett.* **38**, 565 (1997).
- [12] E. Luijten, K. Binder, and H. W. J. Blöte, *Eur. Phys. J. B* **9**, 289 (1999).
- [13] J. L. Jones and A. P. Young, *Phys. Rev. B* **71**, 174438 (2005).
- [14] J. Rudnick, G. Gaspari, and V. Privman, *Phys. Rev. B* **32**, 7594 (1985).
- [15] B. Berche, R. Kenna, and J.-C. Walter, *Nucl. Phys. B* **865**, 115 (2012).
- [16] R. Kenna and B. Berche, *Condens. Matter Phys.* **16**, 23601 (2013).
- [17] P. G. Watson, in *Phase Transitions and Critical Phenomena*, edited by C. Domb and M. Green (Academic, London, 1973), Vol. 2, p. 101.
- [18] E. Brézin, *J. Phys. (Paris)* **43**, 15 (1982).
- [19] J. Shapiro and J. Rudnick, *J. Stat. Phys.* **43**, 51 (1986).
- [20] Equation (22) of Ref. [19] and Eq. (37) of Ref. [18] correspond to Eq. (12) with $\tilde{X}(x, y) = (x + y^2)^{-1}$ at least above T_c . (Below T_c the spherical model behaves quite differently from the Ising model.)
- [21] The spherical model, in which the length constraint $S_i^2 = 1$ on each spin is replaced by a *single* global average constraint, is equivalent to an n -component vector model in the limit of $n \rightarrow \infty$ for the case of periodic boundary conditions. For free boundary conditions, however, the correspondence does not hold. In that case, due to a lack of translational invariance, one would need a *different* average constraint on each spin to reproduce the results of a vector model with an infinite number of components.
- [22] R. Kenna and B. Berche, *Europhys. Lett.* **105**, 26005 (2014).
- [23] U. Wolff, *Phys. Rev. Lett.* **62**, 361 (1989).
- [24] This expression differs from the standard expression for the susceptibility $\chi = \beta L^d (\langle m^2 \rangle - \langle m \rangle^2)$ in two ways. The first trivial difference is that we omit the factor of β which is conventional in critical phenomena studies. Secondly, and not so trivially, we ignore the subtracted term, which is hard to compute reliably by the Monte Carlo method since one would have to apply a field h and take the limit $h \rightarrow 0$ after the limit $L \rightarrow \infty$. Hence the quantity we call χ is really only the susceptibility above T_c . It is, nonetheless, a convenient quantity to study, and it has the claimed scaling behavior.
- [25] W. H. Press, S. A. Teukolsky, W. T. Vetterling, and B. P. Flannery, *Numerical Recipes in C*, 2nd ed. (Cambridge University Press, Cambridge, 1992).
- [26] H. G. Ballesteros, L. A. Fernandez, V. Martin-Mayor, J. Pech, and A. Muñoz Sudupe, *Phys. Lett. B* **378**, 207 (1996).
- [27] M. P. Nightingale, *Physica A* **83**, 561 (1976).
- [28] H. G. Ballesteros, L. A. Fernández, V. Martin-Mayor, A. Muñoz Sudupe, G. Parisi, and J. J. Ruiz-Lorenzo, *Phys. Rev. B* **58**, 2740 (1998).
- [29] M. Weigel and W. Janke, *Phys. Rev. Lett.* **102**, 100601 (2009).
- [30] M. E. J. Newman and G. T. Barkema, *Monte Carlo Methods in Statistical Physics* (Oxford University Press, New York, 1999).
- [31] A. P. Young, [arXiv:1210.3781](https://arxiv.org/abs/1210.3781).
- [32] P. H. Lundow and K. Markström, [arXiv:1408.5509](https://arxiv.org/abs/1408.5509).